Original Research

Revista Brasileira de Física Médica (2026) 20:894

MRI texture changes in young adults undergoing a moderate-intensity running training program

Mateus S. Bonadia[1], Rafael V. da Silveira[1], Gabriela Castellano[1,2]

[1]Instituto de Física Gleb Wataghin, Universidade Estadual de Campinas (UNICAMP), Campinas, SP, Brasil
[2]Brazilian Institute of Neuroscience and Neurology (BRAINN), Campinas, SP, Brasil

Abstract

Several studies have shown structural brain changes resulting from physical exercise. White and gray matter volumes have been reported to increase as a result of physical training in healthy individuals, and a reduction in brain structure atrophy has also been associated with physical activity. However, the assessment of magnetic resonance imaging (MRI) texture changes related to physical exercise has not been investigated. This study aimed to evaluate texture-based structural brain changes in initially sedentary young (< 30 years) participants who completed a moderate-intensity running training program. Structural MR images were obtained before and after the program. Texture features were extracted using the Gray-Level Co-occurrence Matrix (GLCM) and compared between time points to verify changes due to aerobic physical activity. The correlation parameter significantly increased for the left globus pallidus after the intervention. Non-significant trends toward increased correlation were also observed for the right globus pallidus, left hippocampus, right cerebellum, and left precentral gyrus, whereas a decreasing trend was observed for the right inferior frontal gyrus. These findings suggest that texture analysis may be a useful approach for detecting subtle changes in brain MRI associated with cardiovascular exercise in young adults and support further investigation of exercise-related neuroplastic adaptations.

Keywords: Magnetic Resonance Imaging; Exercise; Brain; Texture Analysis; Physical Fitness.

1. Introduction

Neurological magnetic resonance imaging (MRI) provides valuable information for studies of brain structure and function. Particularly, MRI has been used to investigate brain changes resulting from physical exercise programs, both in health and disease (1-4). Functional MRI (fMRI) studies have consistently shown exercise-related alterations in brain activity patterns, task efficiency, and connectivity between regions, particularly in the frontal and parietal cortex and sensorimotor areas, often accompanied by measured improvements in executive function, spatial learning, and cognitive performance (5-8).

Structural MRI studies have also evaluated exercise-related brain changes. Previous investigations in this area have shown increased gray and white matter volumes, reduced brain atrophy and lesions, and preserved cortical structures, along with exercise-associated changes in regions such as the hippocampus, frontal cortex, cerebellum, and other cortical areas in cardiovascular training groups (5,8-16). Overall, these studies suggest that physical activity contributes to structural changes in the brain.

Both functional and structural MRI studies have provided evidence that physical activity promotes measurable changes in the brain. Together, these findings support the concept of exercise-induced neuroplasticity and demonstrate the potential of MRI to investigate brain changes related to exercise. Nevertheless, the structural studies' findings focused primarily on morphometric analyses, which may not fully characterize exercise-induced brain adaptations.

Morphometric analyses have indicated that large-scale measurements of brain structure can reveal how exercise impacts the brain. However, these measurements typically reflect later changes. Early changes in the brain, such as the growth of new blood vessels, the branching of nerve cells, and the formation of new connections, likely happen before any noticeable increase in brain volume. Unfortunately, there is limited research using MRI texture analysis to identify these early changes induced by physical exercise. This study aimed to address that gap by examining texture-based changes in the brains of young adults who were initially inactive and then engaged in a moderate-intensity running program. We hypothesized that texture analysis could effectively detect early signs of brain changes related to exercise.

Texture analysis of an image involves extracting parameters that describe gray-level intensities and their spatial relationships, and it is commonly applied in studies of brain lesions and tumors, particularly in early stages (17-19). In this work, distributions of gray levels in the images were assessed using the Gray-Level Co-occurrence Matrix (GLCM) method, since variations in these values indicate changes in the voxel patterns, which could reflect structural alteration of the underlying brain tissues.

2. Subjects, Materials and Methods

2.1. Subjects

Twenty-two men with ages between 20 and 31 (mean age 24.5 ± 3.4) years participated in this study. Data were collected in a previous study by Klepits and colleagues (20) and made freely available at the OpenNeuro platform (https://openneuro.org/). Data collection was performed in accordance with relevant guidelines and regulations. Recruited participants were sedentary, i.e., they performed less than 150 min of regular physical exercise or sports activities per week (20). The study design included a baseline period (two weeks with no activity), followed by a first running cycle (3.7 weeks) and a second running cycle (3.3 weeks) (Figure 1). MRI exams were acquired at four time points: T1, just before baseline; T2, between baseline and the first running cycle; T3, between the first and second running cycle; and T4, after the second running cycle, i.e., at the end of the program.

In this study, only data from the T1 and T4 assessments were analyzed, representing the pre- and post-intervention conditions. This approach evaluated the cumulative effect of the complete training protocol rather than the temporal evolution of intermediate changes.

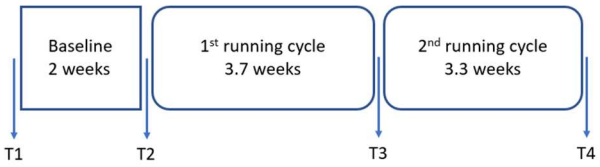

Figure 1. Study design. T1, T2, T3, and T4 indicate assessment moments, including the MRI exams. Only data from T1 and T4 were used in the present study.

2.2. MRI acquisition and processing

Data for this study consisted of three-dimensional (3D) T1 weighted images acquired in a 3T MRI scan (MAGNETOM Vida, Siemens), with the following parameters: TE (time to echo) = 3.9 ms, flip angle = 7˚, TR (time to repetition) = 2.5 s, TI (time to inversion) = 1.2 s, slice thickness = 1 mm, pixel size = 1x1 mm^2; FOV = 256x256 mm^2.

The images were normalized to MNI space using Statistical Parametric Mapping 12 (SPM12) (https://www.fil.ion.ucl.ac.uk/spm/software/spm12/). During preprocessing, tissue segmentation into gray matter, white matter, and CSF was performed, removing non-brain tissues from further processing. Subsequently, the processed images, originally allowing up to 65536 gray levels, were discretized into 64 gray levels to reduce GLCM sparsity. This discretization was performed without intensity normalization based on minimum or maximum voxel values of each image. Although reducing the number of gray levels may cause information loss, sparse GLCMs contain fewer co-occurrences for each voxel-intensity pair, leading to greater uncertainty in the estimated texture features and increased susceptibility to texture noise; therefore, balancing these two factors is important. Then, images were registered to the Anatomical Automated Labeling (AAL) atlas (https://www.gin.cnrs.fr/en/tools/aal/) and parcellated into Regions of Interest (ROIs) (21). These ROIs consisted of atlas-derived masks corresponding to specific brain anatomical structures from which the GLCMs were calculated. This atlas divides the brain into 116 ROIs. To ensure sufficient ROI size and reduce uncertainty in texture estimation, only regions containing more than 900 voxels were considered. For homologous (left-right) regions, if one side contained fewer than 900 voxels, the pair was used only if the contralateral region contained at least 1000 voxels. Applying these criteria reduced the total number of eligible ROIs to 86. From these, we selected nine homologous (left-right) ROI pairs (18 regions) known from the literature to be highly responsive to exercise-induced neuroplasticity. These included 10 regions associated with memory and spatial navigation (e.g., hippocampus), and 8 regions involved in motor control and motor learning (e.g., basal ganglia) (22,23). Due to mask registration anomalies, one homologous ROI from each of two different region pairs was excluded (Right Cerebellum Crus 1 and Left Cerebellum 10), resulting in a final set of 16 ROIs used for analysis. **Erro! Fonte de referência não encontrada.** shows the homologous (left and right) region pairs used as ROIs.

Table 1. AAL ROIs used in the analysis.

AAL region	Anatomical region
L Hippocampus	Left Hippocampus
R Hippocampus	Right Hippocampus
L Precentral	Left Precentral gyrus
R Precentral	Right Precentral gyrus
L Frontal Sup	Left Superior frontal gyrus
R Frontal Sup	Right Superior frontal gyrus
L Frontal Mid	Left Middle frontal gyrus
R Frontal Mid	Right Middle frontal gyrus
L Frontal Inf Oper	Left Inferior frontal gyrus
R Frontal Inf Oper	Right Inferior frontal gyrus (Frontal cortex)
L Pallidum	Left Globus pallidus
R Pallidum	Right Globus pallidus (Basal ganglia)
L Caudate	Left Caudate nucleus
R Caudate	Right Caudate nucleus (Basal ganglia)
L Cerebellum Crus 1	Left Cerebellar crus 1
R Cerebellum 10	Right Cerebellar flocculonodular lobe (Cerebellum)

Source: The author (2026).

Image processing to register the MRI scans to the atlas mask space (voxel size 2x2x2 mm^3; 91x109x91 voxels) was performed using SPM12. This step involved matrix interpolation and applying the normalization field to adjust image resolution to match the mask resolution (intensity and spatial). It is called "coregistering the image to the mask". Coregistered images were further visually inspected to ensure the absence of coregistration misalignments or artifacts.

Subsequently, GLCMs and their parameters were calculated using a MATLAB native function, and the resulting data were analyzed using Python and its libraries NumPy, SciPy, and Pandas (24-26).

2.3. Texture Analysis

In general terms, for a 3D input image, the GLCM is defined as a matrix $M(i,j)$ computed from the original image $L(x,y,z)$ (or from the ROI), where (x,y,z) and (i,j) represent the positions of the elementary units of the image and the entries of GLCM, respectively, as follows:

$$M(i,j)=\sum_{x=1}^{n_1}\sum_{y=1}^{n_2}\sum_{z=1}^{n_3}\begin{cases}1, \text{ if } L(x,y,z)=i \\ \text{and } L(x+dx,\, y+dy,\, z+dz)=j \\ 0, \text{ otherwise}\end{cases} \quad (1)$$

That is, $M(i,j)$ counts the number of times that, given a reference voxel with intensity $L(x,y,z) = i$, there was a voxel at a certain relative position such that $L(x+dx, y+dy, z+dz) = j$. The relative positions of the secondary voxels with respect to the reference voxel may vary according to the analysis requirements and are referred to as the reference voxel's neighborhood. In this study, an isotropic neighborhood defined as a cubic shell centered on the primary voxel was considered. The distances from the center to the sides of this cube varied from 1 to 3 voxels. Only voxel pairs entirely contained within each ROI were used for the GLCM computation.

From the GLCM, Haralick et al. (27) described a set of texture parameters that can be extracted, of which the following were computed in the present study: contrast, entropy, sum entropy, and correlation (see the Appendix).

In summary, for each input image, GLCMs were computed for the three voxel distances for every ROI, from which the texture parameters were extracted, yielding a total of 12 texture parameters per ROI, or 192 texture parameters per image.

2.4. Statistical Analysis

First, the Shapiro normality test was used to verify the normality of the parameters' distributions. Given that they were not normal, the Wilcoxon Signed-Rank Test, a paired non-parametric test, was used to assess possible texture changes resulting from the training program. The significance level adopted was 5%. Additionally, a Bonferroni correction for multiple comparisons was performed, considering four parameters, three GLCM distances, and 16 ROIs, yielding 192 tests.

3. Results

Among all evaluated parameters, only correlation showed significant results; therefore, only this parameter is presented here.

Figures 2 to 7 show the results corresponding to the ROIs for which the correlation parameter was either significantly different (corrected $p < 0.05$) or showed a tendency to be different (uncorrected $p < 0.05$) between instances (T1 and T4). In these plots, the uncorrected p-value is indicated as "p (uncorr.)", while the Bonferroni-corrected p-value is shown as "p".

Only the correlation parameter in the left globus pallidus at a two-voxel distance demonstrated a statistically significant change ($p = 0.02$, corrected) between T1 and T4 (Figure 2). The mean correlation value increased from 0.09 ± 0.04 at T1 to 0.12 ± 0.06 at T4.

Secondary exploratory analyses of the uncorrected data revealed nominal variations (uncorrected $p < 0.05$) in other regions. An increasing trend in correlation values was also observed in the left hippocampus (Figure 3), right globus pallidus (Figure 4), left precentral gyrus (Figure 5), and cerebellum (Figure 7) across all three voxel distances. In contrast, the right inferior frontal gyrus (Figure 6) showed a decreasing trend in correlation values.

Regardless of the changes between T1 and T4, correlation values consistently decreased as voxel distance increased across all evaluated ROIs.

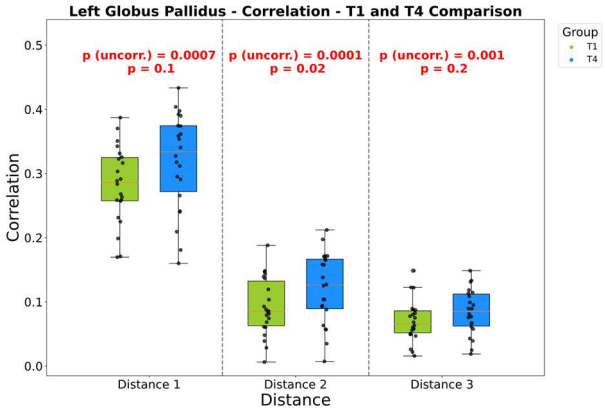

Figure 2. Correlation parameter comparison between T1 and T4 assessments for the three voxel distances for the left globus pallidus. In red, "p (uncorr.)" indicates the uncorrected p-value and "p" the Bonferroni-corrected p-value.

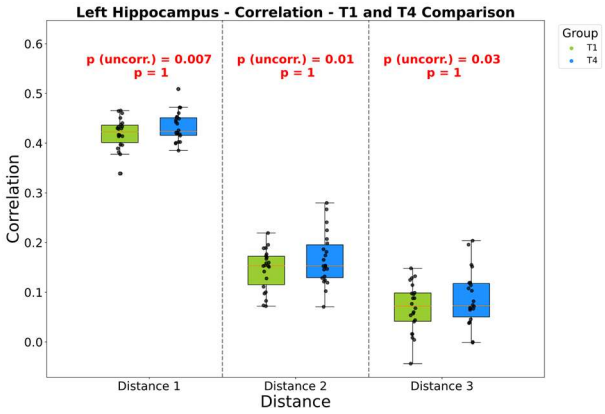

Figure 3. Correlation parameter comparison between T1 and T4 assessments for the three voxel distances for the left hippocampus. In red, "p (uncorr.)" indicates the uncorrected p-value and "p" the Bonferroni-corrected p-value.

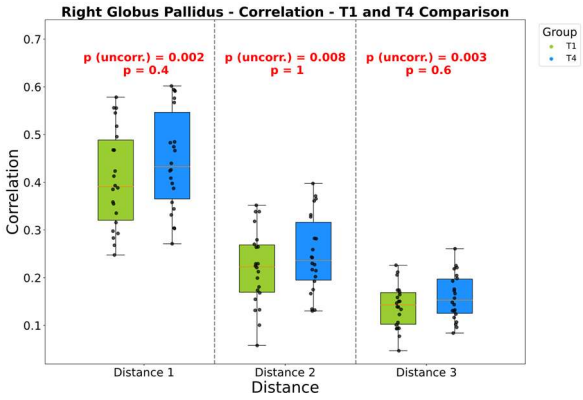

Figure 4. Correlation parameter comparison between T1 and T4 assessments for the three voxel distances for the right globus pallidus. In red, "p (uncorr.)" indicates the uncorrected p-value and "p" the Bonferroni-corrected p-value.

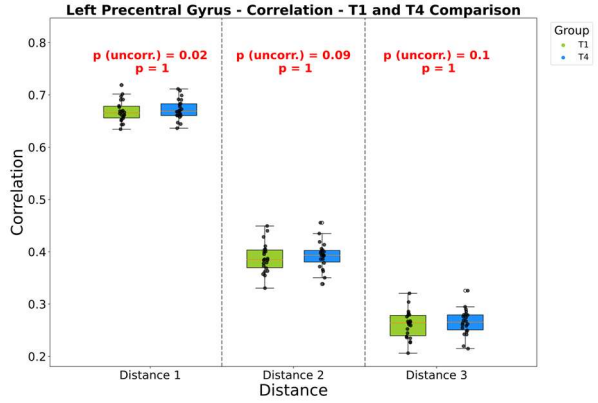

Figure 5. Correlation parameter comparison between T1 and T4 assessments for the three voxel distances for the left precentral gyrus. In red, "p (uncorr.)" indicates the uncorrected p-value and "p" the Bonferroni-corrected p-value.

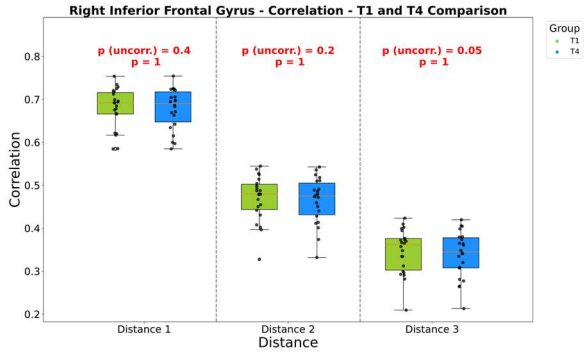

Figure 6. Correlation parameter comparison between T1 and T4 assessments for the three voxel distances for the right inferior frontal gyrus. In red, "p (uncorr.)" indicates the uncorrected p-value and "p" the Bonferroni-corrected p-value.

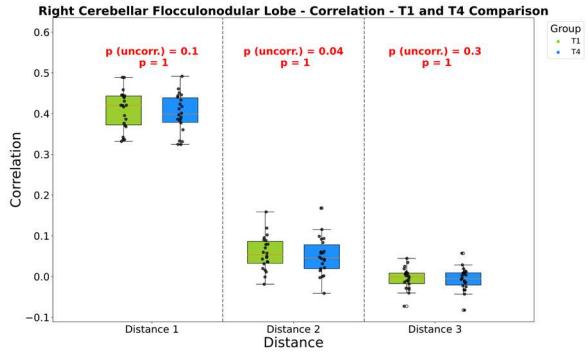

Figure 7. Correlation parameter comparison between T1 and T4 assessments for the three voxel distances for the right cerebellar flocculonodular lobe. In red, "p (uncorr.)" indicates the uncorrected p-value and "p" indicates the Bonferroni-corrected p-value.

4. Discussion

The primary finding of this study was a significant texture difference in the left globus pallidus between T1 and T4 assessments for the GLCM distance 2 (Fig. 2). While not reaching statistical significance after multiple comparison corrections, trends indicating possible texture changes were also observed across all three GLCM voxel distances, for the left and right globus pallidus (Figs. 2 and 4) and left hippocampus (all voxel distances) (Fig. 3); left frontal lobe for distance 1 (Fig. 5); right frontal lobe (Fig. 6) for distance 3, and cerebellum (Fig. 7) for distance 2. While these uncorrected findings do not survive multiple comparison penalties and must be interpreted with caution, they point to target regions for future hypothesis-driven investigations.

Notably, the correlation parameter decreased with increasing voxel distance for the GLCM. This behavior comes from the fact that greater separation distances between voxel pairs reduce their probability of being part of the same anatomical structure. Despite this trend, correlation values showed an increase between T1 and T4 for most ROIs (except for the Right inferior frontal gyrus) across all distances. The interpretation of this texture feature is not straightforward, since it can be influenced by multiple image characteristics. In this study, however, the absence of significant changes in entropy and contrast, for example, suggests that the observed increase in correlation was not accompanied by broader alterations in the texture features evaluated.

This pattern indicates that voxel intensities became more spatially related over the training period, while overall gray-level distributions remained largely unchanged. Such findings suggest that texture analysis may capture subtle image alterations that are not reflected by other texture features evaluated in the present study.

This finding is particularly interesting in the increase in correlation observed in the left globus pallidus, as it is consistent with previous reports describing exercise-related increases in basal ganglia (a macro region associated with the globus pallidus) volume following cardiorespiratory training (19). As the globus pallidus plays an important role in motor control and executive functions (such as working memory and controlling body and eye movement), the texture changes shown may represent a counterpart to adaptations previously identified through morphometric approaches (28).

Although the cerebellum, hippocampus, and motor cortex (precentral gyrus and inferior frontal lobe) did not show statistically significant results after correction for multiple comparisons, exploratory trends observed in these structures are noteworthy as the regions align with existing literature findings on exercise-induced neuroplasticity. As previous studies have reported physical activity-related increases in gray matter volume in the cerebellum and hippocampus, as well as enhanced neuroplasticity in the motor cortex (12,29-32). Rather than providing evidence of structural alterations in these regions, the present findings should be viewed as preliminary observations that warrant further investigation.

Finally, although this study found exercise-induced texture changes on MRI images of the brain, exercise-induced neuroplasticity processes (such as synaptogenesis and angiogenesis) cannot be directly identified as the mechanisms underlying these texture changes. Therefore, any biological interpretation remains speculative and should be confirmed by

future studies combining texture analysis with complementary biological measures and physiological markers of training adaptation.

Much of the literature relating basal ganglia adaptations to aerobic exercise has focused on populations undergoing substantial brain remodeling, such as children, preadolescents, and older adults, whereas the present study evaluated young adults (33-35). In addition, the relatively small sample size of the present study (22 participants) should be considered when interpreting these findings, and larger cohorts are necessary to confirm the observed trends and evaluate their reproducibility.

5. Conclusion

Texture analysis of MRI images using GLCM can reveal image features imperceptible to the human eye, yet it remains relatively unexplored in exercise neuroimaging. In this study, we successfully applied this technique to evaluate brain MRI changes in initially sedentary young adults following a moderate-intensity running program.

Our primary finding is a statistically significant increase in the correlation parameter for the left globus pallidus, suggesting changes in the spatial relation among neighboring voxels that may reflect subtle adaptations associated with the physical activity.

Exploratory analyses also highlighted nominal alterations in the hippocampus, right globus pallidus, and cerebellum. While these latter results remain preliminary and require confirmation in larger, controlled cohorts, our findings support the potential of GLCM-based texture analysis to detect subtle exercise-related brain alterations.

Most existing research verifying anatomical changes in physically active individuals focuses on older adults and early elderly (mean age > 60 years). Our findings suggest that texture analysis may also provide useful information for studying subtle changes in younger adults.

However, the relationship between texture parameters and their underlying biological and anatomical correlates remains complex and not yet fully understood. Therefore, the textural variations and trends observed in this context should be further investigated using larger cohorts and other texture analysis methods, particularly directional ones, such as Run Length matrices.

Overall, the study objective was achieved, and our conclusions support the potential of texture parameters as a complementary approach for investigating structural adaptations associated with physical activity.

6. Future Perspectives

Building on these findings, future studies should explore directional texture analysis methods, such as the Gray-Level Run-Length Matrix (GLRM). Investigating texture directionality could provide deeper insights into the specific architectural reorganization of the basal ganglia and its relation to exercise-induced neuroplasticity.

Acknowledgements

This research was supported by Brazilian Coordination for the Improvement of Higher Education Personnel (CAPES) - Finance Code 001; São Paulo Research Foundation (FAPESP), Grants 2024/03158-9, 2013/07559-3 (BRAINN) and 2024/00998-6 (CRISQuaM); Brazilian National Council for Scientific and Technological Development (CNPq), Grants 306255/2024-3 and 408389/2024-9 (INCT-NeuroComp); and Funding Authority for Studies and Projects (FINEP), Grant 2140/22.

A. Appendix – Texture parameters' formulae

Normalization by pair probability

$$P(i,j)= \frac{M(i,j)}{\sum_{i=1}^{N}\sum_{j=1}^{N} M(i,j)} \quad (2)$$

X weighted sum

$$\mu_x = \sum_{i=1}^{N} i \sum_{j=1}^{N} P(i,j) \quad (3)$$

Y weighted sum

$$\mu_y = \sum_{j=1}^{N} j \sum_{i=1}^{N} P(i,j) \quad (4)$$

X standard deviation

$$\sigma_x^2 = \sum_{i=1}^{N}\sum_{j=1}^{N} P(i,j)(i-\mu_x)^2 \quad (5)$$

Y standard deviation

$$\sigma_y^2 = \sum_{j=1}^{N}\sum_{i=1}^{N} P(i,j)(j-\mu_y)^2 \quad (6)$$

Correlation: Measures how well two voxels are correlated, based on their deviation from the mean distribution

$$Corr = \sum_{i=1}^{N}\sum_{j=1}^{N} \frac{P(i,j)(i-\mu_x)(j-\mu_y)}{\sigma_x \sigma_y} \quad (7)$$

Entropy: Measures the pixel pair intensity randomness

$$\text{Entr}=-\sum_{i=1}^{N}\sum_{j=1}^{N} P(i,j)\log(P(i,j)) \quad (8)$$

Contrast: measures the overall gradient of the image for voxel pairs

$$\text{Cont}=\sum_{i=1}^{N}\sum_{j=1}^{N} P(i,j)(i-j)^2 \quad (9)$$

Sum vector: s = i+j

$$P(s)=\sum_{i=1}^{N}\sum_{j=1}^{N} P(i,j) \quad (10)$$

Entropy of the sum: measures the entropy of the gray-level sum of each voxel pair

$$\text{EntrSum}=-\sum_{s=2}^{2N} P(s)\log(P(s)) \quad (11)$$

References

1. Herold F, Törpel A, Schega L, et al. Functional and/or structural brain changes in response to resistance exercises and resistance training lead to cognitive improvements – a systematic review. Eur Rev Aging Phys Act. 2019;16:10.
2. Johansson H, Hagströmer M, Grooten WJA, Franzén E. Exercise-induced neuroplasticity in Parkinson's disease: a metasynthesis of the literature. Neural Plast. 2020;2020:8961493.
3. Hortobágyi T, Vetrovsky T, Balbim GM, Silva NCBS, Manca A, Deriu F, et al. The impact of aerobic and resistance training intensity on markers of neuroplasticity in health and disease. Ageing Res Rev. 2022;80:101698.
4. Venegas-Sanabria LC, Cavero-Redondo I, Martínez-Vizcaino V, et al. Effect of multicomponent exercise in cognitive impairment: a systematic review and meta-analysis. BMC Geriatr. 2022;22:617.
5. Colcombe SJ, Erickson KI, Scalf PE, Kim JS, Prakash R, McAuley E, et al. Aerobic exercise training increases brain volume in aging humans. J Gerontol A Biol Sci Med Sci. 2006;61(11):1166-70.
6. Holzschneider K, Wolbers T, Röder B, Hötting K. Cardiovascular fitness modulates brain activation associated with spatial learning. Neuroimage. 2012;59(3):3003-14.
7. Voelcker-Rehage C, Godde B, Staudinger UM. Cardiovascular and coordination training differentially improve cognitive performance and neural processing in older adults. Front Hum Neurosci. 2011;5:26.
8. Johansson ME, Cameron IGM, Van der Kolk NM, de Vries NM, Klimars E, Toni I, et al. Aerobic exercise alters brain function and structure in Parkinson's disease: a randomized controlled trial. Ann Neurol. 2022;91(2):203-16.
9. Benedict C, Brooks SJ, Kullberg J, Nordenskjöld R, Burgos J, Le Grevès M, et al. Association between physical activity and brain health in older adults. Neurobiol Aging. 2013;34(1):83-90.
10. Gow AJ, Bastin ME, Muñoz Maniega S, Valdés Hernández MC, Morris Z, Murray C, et al. Neuroprotective lifestyles and the aging brain: activity, atrophy, and white matter integrity. Neurology. 2012;79(17):1802-8.
11. Raji CA, Meysami S, Hashemi S, Garg S, Akbari N, Ahmed G, et al. Exercise-related physical activity relates to brain volumes in 10,125 individuals. J Alzheimers Dis. 2024;97(2):829-39.
12. Erickson KI, Voss MW, Prakash RS, Basak C, Szabo A, Chaddock L, et al. Exercise training increases size of hippocampus and improves memory. Proc Natl Acad Sci U S A. 2011;108(7):3017-22.
13. Pajonk FG, Wobrock T, Gruber O, Scherk H, Berner D, Kaizl I, et al. Hippocampal plasticity in response to exercise in schizophrenia. Arch Gen Psychiatry. 2010;67:133-43.
14. Rovio S, Spulber G, Nieminen LJ, Niskanen E, Winblad B, Tuomilehto J, et al. The effect of midlife physical activity on structural brain changes in the elderly. Neurobiol Aging. 2010;31:1927-36.
15. de Zoete RMJ, Berryman CF, Nijs J, Walls A, Jenkinson M. Differential structural brain changes between responders and nonresponders after physical exercise therapy for chronic nonspecific neck pain. Clin J Pain. 2023;39(6):270-7.
16. Diaz-Galvan P, Franco-Rosado P, Silva-Rodriguez J, Castro-Labrador S, Labrador-Espinosa MA, Muñoz-Delgado L, et al. Association of physical exercise with structural brain changes and cognitive decline in patients with early Parkinson disease. Neurology. 2025;105(5):e213932.
17. Kassner A, Thornhill RE. Texture analysis: a review of neurologic MR imaging applications. AJNR Am J Neuroradiol. 2010;31(5):809-16.
18. Kunimatsu A, Yasaka K, Akai H, Sugawara H, Kunimatsu N, Abe O. Texture analysis in brain tumor MR imaging. Magn Reson Med Sci. 2022;21(1):95-109.
19. Voelcker-Rehage C. Exercise-induced changes in basal ganglia volume and their relation to cognitive performance. J Neurol Neuromedicine. 2016;1(5):19-24.
20. Klepits P, Koschutnig K, Zussner T, Fink A. Effects of a seven-week running intervention with moderate intensity on the volume of the hippocampus and depressive symptoms in young men from the general population. OpenNeuro. 2024;ds004937.v1.0.1.
21. Tzourio-Mazoyer N, Landeau B, Papathanassiou D, Crivello F, Étard O, Delcroix N, et al. Automated anatomical labeling of activations in SPM using a macroscopic anatomical parcellation of the MNI MRI single-subject brain. Neuroimage. 2002;15:273-89.
22. Eichenbaum H. The role of the hippocampus in navigation is memory. J Neurophysiol. 2017;117(4):1785-96.
23. Groenewegen HJ. The basal ganglia and motor control. Neural Plast. 2003;10:108384.
24. Harris CR, Millman KJ, van der Walt SJ, et al. Array programming with NumPy. Nature. 2020;585:357–362.
25. Virtanen P, Gommers R, Oliphant TE, et al. SciPy 1.0: Fundamental algorithms for scientific computing in Python. Nat Methods. 2020;17(3):261–272.
26. McKinney W. Data structures for statistical computing in Python. In: Proceedings of the 9th Python in Science Conference. 2010. p. 56–61.
27. Haralick RM, Shanmugam K, Dinstein I. Textural features for image classification. IEEE Trans Syst Man Cybern. 1973;SMC-3(6):610-21.
28. Arsalidou M, Duerden EG, Taylor MJ. The centre of the brain: topographical model of motor, cognitive, affective, and somatosensory functions of the basal ganglia. Hum Brain Mapp. 2013;34(11):3031-54.
29. Jalanko P, Säisänen L, Kallioniemi E, Könönen M, Lakka TA, Määttä S, et al. Associations between physical fitness and cerebellar gray matter volume in adolescents. Scand J Med Sci Sports. 2024;34(1):e14513.
30. Cherednichenko A, Miró-Padilla A, Adrián-Ventura J, Monzonís-Carda I, Beltran-Valls MR, Moliner-Urdiales D, et al. Physical activity and hippocampal volume in young adults. Brain Imaging Behav. 2024;18(6):1333-42.
31. Klepits P, Koschutnig K, Zussner T, Fink A. Changes in hippocampal volume and affective functioning after a moderate intensity running intervention. Brain Struct Funct. 2024;230(1):2.
32. Lulic T, El-Sayes J, Fassett HJ, Nelson AJ. Physical activity levels determine exercise-induced changes in brain excitability. PLoS One. 2017;12(3):e0173672.
33. Nagamatsu LS, Weinstein AM, Erickson KI, Fanning J, Awick EA, Kramer AF, et al. Exercise mode moderates the relationship between mobility and basal ganglia volume in healthy older adults. J Am Geriatr Soc. 2016;64(1):102-8.
34. Chaddock L, Erickson KI, Prakash RS, VanPatter M, Voss MW, Pontifex MB, et al. Basal ganglia volume is associated with

aerobic fitness in preadolescent children. Dev Neurosci. 2010;32(3):249-56.
35. Loprinzi PD, Roig M, Etnier JL, Tomporowski PD, Voss M. Acute and chronic exercise effects on human memory: what we know and where to go from here. J Clin Med. 2021;10(21):4812.

Contact:

Mateus Santos Bonadia
Universidade de Campinas (UNICAMP)
Rua Sergio Buarque de Holanda, 777
Cidade Universitária Zeferino Vaz
Barão Geraldo, Campinas - SP, 13083-859, Brasil.
mateusbonadia@gmail.com